

Published in final edited form as:

J Med Chem. 2007 July 12; 50(14): 3380–3387. doi:10.1021/jm0704671.

Quick Assembly of 1,4-Diphenyltriazoles as Probes Targeting β -Amyloid Aggregates in Alzheimer's Disease

 Wenchao Qu[†], Mei-Ping Kung[†], Catherine Hou[†], Shunichi Oya[†], and Hank F. Kung^{*,†,‡}

Departments of Radiology and Pharmacology, University of Pennsylvania, Philadelphia, Pennsylvania 19104

Abstract

Accumulation of β -amyloid aggregates ($A\beta$) in the brain is linked to the pathogenesis of Alzheimer's disease (AD). We report a novel approach for producing 1,4-diphenyltriazoles as probes for targeting $A\beta$ aggregates in the brain. The imaging probes, a series of substituted tricyclic 1,4-diphenyltriazoles showing excellent binding affinities to $A\beta$ aggregates ($K_i = 4\text{--}30$ nM), were conveniently assembled by "click chemistry." Two radioiodinated probes, [¹²⁵I]**10a** and [¹²⁵I]**10b**, and two radiofluorinated probes, [¹⁸F]**17a** and [¹⁸F]**17b**, exhibited moderate lipophilicities and showed excellent initial brain penetrations and fast washouts from the normal mouse brain. In vitro autoradiography of postmortem AD brain sections and homogenates showed that these triazoles were binding to $A\beta$ plaques. Preliminary results strongly suggest that use of click chemistry, which led to a 1,4-diphenyltriazole-based core, is a highly convenient and flexible approach for assembling novel imaging agents for targeting $A\beta$ aggregates in senile plaques in the living human brain.

Introduction

Alzheimer's disease (AD)^a is a neurodegenerative disorder of the brain predominantly affecting the older population. Diagnosis of this disease is based on neurological observations, which are often difficult and unreliable. There is an urgent unmet need for specific probes targeting markers in the brain, which can facilitate the diagnosis of this disease. It is generally believed that the accumulation of β -amyloid ($A\beta$) aggregates (major protein aggregates of senile plaques) in the brain is the hallmark of AD.^{1–3} Probes targeting these $A\beta$ aggregates in the brain may greatly facilitate the diagnosis of AD. Indeed, radionuclide-labeled agents targeting the $A\beta$ aggregates have already been developed.^{4,5} A diverse group of core structures (Figure 1) have demonstrated high in vivo and in vitro binding to the $A\beta$ aggregates present in the AD brain, including 4-*N*-methylamino-4'-hydroxystilbene (**1**, SB-13),^{6,7} 6-iodo-2-(4'-dimethylamino)phenyl-imidazo[1,2-*a*]pyridine (**2**, IMPY),^{8,9} and 2-(4'-methylaminophenyl)-6-hydroxybenzothiazole (**3**, PIB).^{10,11} 2-[1-(6-

© 2007 American Chemical Society

^{*}Corresponding author: Department of Radiology, University of Pennsylvania, 3700 Market Street, Room 305, Philadelphia, PA 19104; tel (215) 662-3096; fax (215) 349-5035; kunghf@sunmac.spect.upenn.edu.

[†]Department of Radiology.

[‡]Department of Pharmacology.

 Supporting Information Available: Procedures for synthesizing some intermediates; elemental analysis results and HPLC purity analysis data for all bioassay-involved compounds in two different HPLC systems; and full sets of biodistribution data in normal mice for [¹²⁵I]**10a**, [¹²⁵I]**10b**, [¹⁸F]**17a**, and [¹⁸F]**17b**. This material is available free of charge via the Internet at <http://pubs.acs.org>.

^aAbbreviations: SPECT, single photon emission computed tomography; PET, positron emission tomography; AD, Alzheimer's disease; $A\beta$, β -amyloid; PIB, 2-(4'-methylaminophenyl)-6-hydroxybenzothiazole; SB-13, 4-*N*-methylamino-4'-hydroxystilbene; FDDNP, 2-[1-(6-(2-fluoroethyl)(methyl)-amino)naphthalen-2-yl)ethylidene]malononitrile; IMPY, 6-iodo-2-(4'-dimethylamino-)phenylimidazo[1,2-*a*]pyridine; CuAAC, Cu(I)-catalyzed azide-alkyne cycloaddition; PC, partition coefficient.

[(2-Fluoroethyl)(methylamino)naphthalen-2-yl]ethylidene]-malononitrile (**4**, FDDNP)^{12,13} binds to both plaques and tangles (τ aggregates). Additional core structures have been reported,^{5,10,14–21} suggesting that there are a number of potential small molecules that can fit into the binding pockets of $A\beta$ aggregates in the senile plaques of AD patients. It is generally assumed that the *p*-*N*-methyl- or *p*-*N,N*-dimethylaminophenyl-group is critical for successful binding affinity. Modifications of the phenyl group on the other end of structures **1–3** are tolerated and may not alter the binding affinity.

Recently, we have reported a series of novel tricyclic 2,5-diphenylthiophene derivatives, **5a–d**, that contain a *p*-*N*-methyl- or *p*-*N,N*-dimethylaminophenyl- group (Figure 2).²² Some of these diphenylthiophene compounds displayed excellent binding affinities (ranging from 3.9 to 31 nM, depending on the substitution patterns on the phenyl ring). The fluoroethyl-substituted 2,5-diphenylthiophene, **5c**, showed excellent binding affinity. However, due to the high lipophilicity associated with thiophenes, they were not evaluated further. To reduce the lipophilicity, we modified the thiophene ring by substituting the ring with triazoles, which can be quickly assembled by “click chemistry”. The use of “click chemistry”, modified Huisgen condition,²³ to quickly assemble various interesting molecules has attracted a lot of interest as an approach for drug development.^{24–30} Click chemistry reactions, which commonly employ a Cu(I)-catalyzed azide–alkyne cycloaddition (CuAAC), have several distinctive advantages, including use of modular and fragment-based reagents, wide scope, stereospecificity, easy separation, and high yield.^{31–33} Resveratrol, **6**, is a natural antioxidant normally present in red wine, which may modify the metabolism of lipoproteins and may have beneficial effects of antioxidants.²⁹ A group of compounds, **7**, triazole-modified analogues of **6**, were prepared by click chemistry and tested (Figure 2). This quick assembly method is particularly suited for generating diversified substitution groups and developing novel agents for studying biologically important processes and targeted binding sites. The reaction shows great promise for discovery applications because it combines the synthesis and screening of libraries, which can be done by microfluidics.^{24,34}

Recently, “hot click reactions” have been applied in the preparation of radiopharmaceuticals in situ.^{35–37} In these reports, radiolabeling fragments were “clicked” to form the F-18 labeled radiopharmaceuticals. Besides, the click reaction have also been utilized to assemble the chelates, which were further used for the radiolabeling.^{38,39} Herein we used “cold” click chemistry to assemble a novel series of diphenyltriazoles as probes for the investigation of specific binding site(s) on $A\beta$ protein aggregates. Following a “cold” click approach, several diphenyltriazole derivatives as analogues of stilbenes (previously tested $A\beta$ plaque-specific imaging agents) were prepared, subsequently radiolabeled, and evaluated as potential candidates for positron emission tomography (PET) or single photon emission computerized tomography (SPECT) imaging of amyloid plaques.

Chemistry

The rationale for using “cold” click chemistry for developing new radiopharmaceuticals is based on several unique features: (1) synthesis can be broken down to fragments and the key assembling step can readily be accomplished by “click” reaction; (2) the reaction can be adapted to fragments with various substitution groups and therefore facilitate the assembly of diversified groups of substituting groups; (3) the core structure (tricyclic ring system of diphenyltriazole) contains three nitrogens, which reduce the lipophilicity as compared to thiophene analogues; (4) additional variations of the triazole ring, containing combinations of an assortment of nitrogen and oxygen atoms, may further extend the range of five-membered rings suitable for providing probes with high binding affinities; and (5) various

substitution groups on the tricyclic ring systems may modulate the biological kinetics, thus leading to probes with improved signal-to-noise ratios in PET or SPECT imaging.

The Cu-catalyzed method reported by Sharpless and coworkers²⁸ was introduced to assemble the iodinated ligands **10a** (70%) and **10b** (98%) (Scheme 1). A combination of copper(II) sulfate/sodium ascorbate was utilized in situ to prepare the copper(I) species, and a “click reaction” was achieved in 1 day at the room temperature. Subsequently, a palladium-catalyzed trans-stannylation afforded the tributyltin precursors **11a** and **11b** for radiolabeling with 45% and 66% yields, respectively. In order to radioiodinate the ligands, the standard iododestannylation reactions, using sodium [¹²⁵I]iodide, hydrogen peroxide, and hydrochloric acid, were successfully applied to yield [¹²⁵I]-**10a** and [¹²⁵I]-**10b** with excellent yields (80–85%) and greater than 95% radiochemical purities.

A one-pot two-step approach reported by Fokin and coworkers⁴⁰ was utilized to synthesize the fluoro- and hydroxypegylated diphenyltriazole derivatives **13a,b** (Scheme 2). By directly reacting alkylated iodobenzene **12a,b**, terminal alkyne **8a,b**, and sodium azide in one pot, the desired diphenyltriazoles **13a,b** were synthesized with acceptable yields (62% and 65%). Furthermore, the reaction between **13b** and diethylaminosulfur trifluoride (DAST), which was performed under 0 °C over 0.5 h, provided the fluoropegylated ligand **13c** in 20% yield.

The desired diphenyltriazole derivatives **15a,b** were prepared by a modified one-pot two-step approach (Scheme 3), which was developed by Liang and co-workers.⁴¹ In this reaction, a chelating ligand *trans*-*N,N'*-dimethyl-1,2-cyclohexanediamine, copper(I) iodide, and an equal amount of sodium ascorbate were used as the catalysts. The desired reactions were accomplished at room temperature in 3 h, with yields of 99% and 92%, respectively. The alcohols **15a,b** were then converted to the tosylates **16a,b** (96% and 90%), and a microwave-assisted fluorination reaction afforded final products **17a,b** (80% and 99%).

To obtain [¹⁸F]**17a** and [¹⁸F]**17b**, the corresponding tosylated precursors **16a** and **16b** were reacted with [¹⁸F]fluoride in the presence of Kryptofix 222 and potassium carbonate in DMSO at 120 °C for 4 min. The resulting F-18 labeled crude products were purified by HPLC (Figure 3). The desired products were obtained in 70 min, and the specific activities at the end of synthesis were 600 and 800 mCi/μmol for [¹⁸F]**17a** and [¹⁸F]-**17b**, respectively. The radiochemical purities were >99% for both ligands, and the radiochemical yields were 50% for [¹⁸F]-**17a** and 30% for [¹⁸F]**17b** (decay-corrected).

Biological Studies

Several of the diphenyltriazoles here synthesized displayed excellent to good binding affinities (Table 1). Two iodophenyltriazole derivatives, **10a** and **10b**, effectively competed with [¹²⁵I]**2** binding, showing comparable and lower K_i values of 4.0 ± 0.4 and 8.0 ± 1.6 nM, respectively.

In order to simplify the radiolabeling of F-18 agents and modulate lipophilicity of potential probes targeting A β aggregates, we had previously developed a series of fluoropegylated stilbene and styrylpyridine derivatives.^{18,42,43} The “hot” fluorination reaction can be readily accomplished by a nucleophilic substitution of a mesylated or tosylated terminal leaving group by an activated fluoride ion. When a fluoropegylated chain was added to one end of the phenyl group, it led to two active diphenyltriazoles, **13a** and **13c**. A higher binding affinity was observed for **13c** ($K_i = 8.4 \pm 1.7$ nM) as compared to **13a** ($K_i = 30.0 \pm 6.0$ nM). Compared to **13c**, a slightly lower binding affinity for the hydroxypegylated derivative **13b** was obtained ($K_i = 16.5 \pm 3.3$ nM). Similarly, two fluoroalkyl triazoles **17a** and **17b** had K_i values of 5.0 ± 1.0 and 6.2 ± 1.2 nM, respectively, indicating that they could effectively compete with [¹²⁵I]**2** binding to amyloid plaques. After replacement of the fluoro group of

17a or **17b** with a hydroxy group, the binding affinities of the resulting triazoles showed a slight ($K_i = 10.0 \pm 2.0$ nM for **15a**) to a significant reduction ($K_i = 75.0 \pm 10$ nM for **15b**).

On the basis of the encouraging in vitro binding data obtained for **10a**, **10b**, **17a**, and **17b**, we chose to carry out further biological evaluations on the corresponding I-125 or F-18 labeled probes. It was anticipated that eventually the I-125 or F-18 labeling probes would be suitable for imaging with SPECT or PET. Because the probes need to penetrate the brain easily after iv injection, the partition coefficient (PC, commonly measured as $\log P$) is an important factor for consideration. A moderate lipophilicity ($\log P = 1-3.5$) is highly desirable. The radiofluorinated diphenyltriazoles [^{18}F]**17a** and [^{18}F]**17b** had lower PCs ($\log P = 2.7$ for both) as compared to the two radioiodinated triazoles, [^{125}I]**10a** and [^{125}I]**10b**, which had $\log P$ values of 3.0 and 3.4, respectively. When normal mice were evaluated for whole animal distribution, these radiolabeled triazoles displayed excellent initial brain penetrations (6–9.5% ID/g at 2 min) (Figure 4). The initial high brain uptakes (at 2 min after the injection) observed for these radiolabeled probes, especially for the radioiodinated probes [^{125}I]**10a** and [^{125}I]**10b**, were subsequently followed by rapid washout with less than 0.5% ID/g remaining in the brain at 2 h after the injection. [^{18}F]-**17a** and [^{18}F]**17b** appeared to show fast washouts initially, but this was followed by gradually slower rates of clearance from the mouse brain, resulting in higher residual radioactivities (1–2% ID/g at 2 h after tracer injection). Thus, the two iodinated probes [^{125}I]**10a** and [^{125}I]**10b** had higher and better brain washout indexes ($\text{brain}_{2\text{min}}/\text{brain}_{30\text{min}}$) of 5.66 and 3.72, respectively. [^{18}F]**17a** and [^{18}F]**17b** had lower indexes of 2.34 and 2.31, respectively, which is less favorable for $A\beta$ plaque detection.^{5,10}

It is worth noting that there was a significant amount of in vivo defluorination (reflected by bone uptake) observed with [^{18}F]**17a** (4.64% ID/g, Supporting Information) and [^{18}F]**17b** (18.59% ID/g, Supporting Information). These values are 5–10 times higher as compared to the values reported for previous PET ligands.^{18,20,43} The unfavorable in vivo stability of these two fluoroalkylated triazoles make them less attractive as potential imaging agents. It has been previously demonstrated that F-18 labeled stilbene and styrylpyridine derivatives containing three PEG units are not significantly defluorinated in vivo.^{18,20,42,43} We are currently evaluating [^{18}F]**13c** (which contains three PEG units) as an improved PET imaging agent. The preliminary data clearly indicated the more stable nature of [^{18}F]**13c**. Detailed evaluations of this ligand as a more suitable PET ligand will be reported in a separate publication.

To investigate the ability of these probes to bind with $A\beta$ aggregates in human brain tissues, we have carefully constructed a macroarray block of postmortem human brain samples consisting of seven confirmed AD cases. After sectioning of this macroarray block, adjacent sections, which reflect a comparable pathophysiology, were used. In vitro film autoradiography was carried out using these novel I-125 or F-18 labeled diphenyltriazole probes. Among the probes examined, [^{18}F]**17a** and [^{18}F]**17b** exhibited the most distinctive $A\beta$ plaque-labeling and a minimal level of background in the white matter areas of AD brain (Figure 5). The labeling pattern was consistent with that observed by immunohistochemical labeling with an antibody (4G8) specific for $A\beta$ (data not shown). In addition to plaque labeling, [^{125}I]**10a** displayed significant white matter labeling under a similar incubation condition. A similar pattern was also observed for [^{125}I]**10b** (data not shown). The higher background labeling observed for [^{125}I]**10a** and [^{125}I]**10b** may be related to their higher lipophilicity ($\log P = 3.0$ and 3.4, respectively).

To further characterize the specificity of plaque binding, we evaluated [^{125}I]**10a** and [^{18}F]**17a** with a direct in vitro binding assay using homogenates (from different brain regions) prepared from AD and control brain tissues. For both ligands the signal for specific

binding was detected predominantly in the gray matter homogenates of AD. In contrast, in white matter homogenates of AD brain, the binding signals for both [^{125}I]-**10a** and [^{18}F]**17a** were very low or nonexistent (Figure 6). In the homogenates of control brain tissues (both gray and white matters), the specific binding signal was low, suggesting that the specific binding was highly selective to the AD brain due to the presence of A β plaques in these brain samples.

In conclusion, by use of convenient click chemistry, a series of substituted tricyclic diphenyltriazoles were successfully prepared as potential PET and SPECT imaging agents for targeting A β plaques in the brains of patients with AD. These diphenyltriazole derivatives showed excellent binding affinities to A β plaques (K_i in the nanomolar range). The radiolabeled diphenyltriazoles, especially I-125 labeled **10a** and **10b**, also had very good in vivo properties—high initial uptake and fast washout in normal mice. Specific plaque-binding was clearly delineated by I-125 or F-18 labeled diphenyltriazoles. Taken together, these diphenyltriazole probes demonstrate promising in vitro and in vivo characteristics and they may provide a convenient platform for development of new imaging agents targeting amyloid plaques in the brain.

Experimental Section

General Information

All reagents used were commercial products and were used without further purification unless otherwise indicated. Flash chromatography (FC) was performed on silica gel 60 (230–400 mesh, Sigma–Aldrich). Preparative thin-layer chromatography (PTLC) was performed on silica gel plates with a fluorescent indicator that was visualized with light at 254 nm (Analtech). For each procedure, “standard workup” refers to the following steps: addition of the indicated organic solvent, washing the organic layer with water and then brine, separation of the organic layer from the aqueous layer, drying off the combined organic layers with sodium sulfate or magnesium sulfate, filtering off the solid, and concentrating the filtrate under reduced pressure. Microwave-assisted reactions were performed in a Initiator microwave reactor (Biotage). ^1H NMR spectra were obtained at 200 MHz, and ^{13}C NMR spectra were recorded at 50 MHz (Bruker DPX spectrometer). Chemical shifts were reported as δ values (parts per million) relative to internal tetramethylsilane (TMS). Coupling constants are reported in hertz. The multiplicity is defined by s (singlet), d (doublet), t (triplet), br (broad), or m (multiplet). High-resolution MS experiments were performed at the McMaster Regional Centre for Mass Spectrometry on a Micromass/Waters GCT instrument (GC-EI/CI time-of-flight mass spectrometer). Elemental analyses were performed by Atlantic Microlab INC. Analytical HPLC analysis was carried out on an Agilent 1100 series LC. Two systems were used to confirm the purity of some compounds listed in this section. System A conditions: Phenomenex Gemini $5\mu\text{m}$ C18 110A reverse-phase analytical column (250×4.6 mm, $5\mu\text{m}$), 70/30 $\text{CH}_3\text{CN}/1$ mM ammonium formate (pH = 7) water buffer, 1.0 mL/min, UV 292 nm. System B conditions: Phenomenex silica column (4.6×250 mm, $5\mu\text{m}$), EtOAc/hexanes (from 30/70 to 80/20), 1.0 mL/min, UV 292 nm. All compounds reported in this paper showed greater than 95% purity in both systems.

4-[1-(4-Iodophenyl)-1H-1,2,3-triazol-4-yl]-N-methylbenzenamine (10a)—Alkyne **8a** (0.042 g, 0.32 mmol), azide **9** (0.32 mmol, 0.079 g), and sodium ascorbate (0.16 mL, fresh prepared 1.0 M solution) were added into *t*-butanol/ H_2O (1/1 v/v, 2 mL) and the whole mixture was degassed with nitrogen for 10 min. Copper(II) sulfate (CuSO_4 , 1.0 M aqueous solution, $16\mu\text{L}$) was added and the reaction mixture was vigorously stirred at room temperature (rt) for 24 h. After dilution with ice-cold water (10 mL), the mixture was filtered and washed with cold water and ice-cold Et_2O . The solid was dried under vacuum to

afford **10a** (0.084 g, 70%) as a pale green solid. $^1\text{H NMR}$ $[(\text{CD}_3)_2\text{CO}]$ δ 8.75 (s, 1H), 7.99 (d, 2H, $J = 8.8$ Hz), 7.82–7.72 (m, 4H), 6.69 (d, 2H, $J = 8.7$ Hz), 5.19 (br s, 1H), 2.85, 2.83 (s, 3H, $-\text{NCH}_3$). $^{13}\text{C NMR}$ (DMSO- d_6) δ 150.0, 148.4, 138.5, 136.4, 126.4, 121.6, 117.3, 117.0, 111.7, 93.7, 29.6. HRMS calcd for $\text{C}_{15}\text{H}_{13}\text{IN}_4$ (M^+), 376.0185; found, 376.0168.

4-[1-(4-iodophenyl)-1H-1,2,3-triazol-4-yl]-N,N-dimethylbenzenamine (10b)—

Following the procedure in the preparation of **10a**, compound **10b** was prepared from alkyne **8b** (0.073 g, 0.50 mmol) and **9** (0.147 g, 0.60 mmol) as a pale yellow solid (0.191 g, 98% yield). $^1\text{H NMR}$ $[(\text{CD}_3)_2\text{CO}]$ δ 8.81 (s, 1H), 7.99 (d, 2H, $J = 8.9$ Hz), 7.86–7.73 (m, 4H), 6.84 (d, 2H, $J = 8.9$ Hz), 3.00 (s, 6H). $^{13}\text{C NMR}$ (DMSO- d_6) δ 150.3, 148.1, 138.5, 136.4, 126.2, 121.6, 121.5, 117.7, 117.3, 112.3, 93.8. HRMS calcd for $\text{C}_{16}\text{H}_{15}\text{IN}_4$ (M^+), 390.0341; found, 390.0332. Anal. ($\text{C}_{16}\text{H}_{15}\text{IN}_4$) C, H, N: calcd, 14.36; found, 14.47.

N-Methyl-4-[1-(4-tributylstannylphenyl)-1H-1,2,3-triazol-4-yl]benzenamine (11a)

—A mixture of **10a** (0.041 g, 0.11 mmol), bis(tributyltin) $[(\text{Bu}_3\text{Sn})_2]$ (0.319 g, 0.55 mmol), and palladium tetrakis(triphenyl)phosphine $[\text{Pd}(\text{PPh}_3)_4]$ (0.013 g, 10 mol %) in toluene was heated at 100 °C for 4 h. The reaction solution was cooled to rt and treated with 5 mL of 10% KF. After vigorous stirring for an additional 0.5 h, the standard workup with EtOAc and following PTLC (EtOAc/hexanes, 30/70) afforded **11a** as a pale yellow solid (0.026 g, 45%). $^1\text{H NMR}$ (CDCl_3) δ 8.05 (s, 1H), 7.77–7.70 (m, 4H), 7.62 (d, 2H, $J = 8.3$ Hz), 6.70 (d, 2H, $J = 8.6$ Hz), 3.86 (br s, 1H), 2.91, 2.90 (s, 3H, $-\text{NCH}_3$), 1.66–1.50 (m, 6H), 1.45–1.27 (m, 6H), 1.15–1.01 (m, 6H), 0.91 (t, 9H, $J = 7.2$ Hz). $^{13}\text{C NMR}$ (CDCl_3) δ 149.7, 149.1, 143.4, 138.1, 137.8, 137.4, 137.3, 127.2, 120.3, 119.9, 119.6, 119.5, 116.1, 112.7, 30.8, 29.5, 29.3, 29.1, 28.1, 27.5, 27.0, 13.9, 13.4, 13.2, 10.0, 6.7, 6.5. HRMS calcd for $\text{C}_{27}\text{H}_{41}\text{N}_4\text{Sn}$ ($\text{M}^+ + \text{H}^+$), 541.2353; found, 541.2366.

N,N-Dimethyl-4-[1-(4-tributylstannylphenyl)-1H-1,2,3-triazol-4-yl]benzenamine (11b)

—In accordance with the procedure for the preparation of **11a**, compound **11b** was prepared from **10b** (0.039 g, 0.1 mmol) as a light yellow solid (0.037 g, 66% yield). $^1\text{H NMR}$ (CDCl_3) δ 8.06 (s, 1H), 7.81–7.72 (m, 4H), 7.62 (d, 2H, $J = 8.4$ Hz), 6.81 (d, 2H, $J = 8.9$ Hz), 3.02 (s, 6H), 1.66–1.50 (m, 6H), 1.45–1.24 (m, 6H), 1.15–1.02 (m, 6H), 0.91 (t, 9H, $J = 7.1$ Hz). $^{13}\text{C NMR}$ (CDCl_3) δ 150.7, 149.0, 143.4, 138.1, 137.7, 137.4, 137.3, 127.2, 127.0, 120.3, 119.9, 119.5, 118.7, 116.1, 112.7, 40.6, 29.4, 29.2, 29.0, 28.1, 27.5, 26.9, 13.8, 13.3, 13.2, 9.9, 6.7, 6.5. HRMS calcd for $\text{C}_{27}\text{H}_{40}\text{N}_4\text{Sn}$ (M^+), 554.2431; found, 554.2433.

4-(1-[4-(2-[2-(2-Fluoroethoxy)ethoxy]ethoxy)phenyl]-1H-1,2,3-triazol-4-yl)-N-methylbenzenamine (13a)

—To a 20 mL scintillation vial were added alkyne **8a** (0.040 g, 0.3 mmol), iodobenzene **12b** (0.106 g, 0.3 mmol), Na_2CO_3 (0.003 g, 0.03 mmol), L-proline (0.0035 g, 0.003 mmol), NaN_3 (0.029 g, 0.45 mmol), sodium ascorbate (0.006 g, 0.03 mmol), CuSO_4 (1.0 M aqueous solution, 0.015 mL), and 1.0 mL of mixed solvent DMSO and H_2O (9/1 v/v). After being purged by nitrogen 10 min, the reaction mixture was heated to 65 °C for 24 h. It was cooled down to rt, poured into diluted ammonia (20 mL), and extracted with EtOAc (3×15 mL). The combined organic phase was washed with brine (2×10 mL), dried over Na_2SO_4 , filtered, and concentrated. The residue was submitted to FC (EtOAc/hexanes, 70/30) to afford a light brown solid **13a** (0.745 g, 62%). $^1\text{H NMR}$ (CDCl_3) δ 7.97 (s, 1H), 7.76–7.63 (m, 4H), 7.06 (dt, 2H, $J_1 = 9.0$ Hz, $J_2 = 2.7$ Hz), 6.72 (d, 2H, $J = 8.6$ Hz), 4.72–4.68 (m, 1H), 4.49–4.44 (m, 1H), 4.20 (t, 2H, $J = 2.5$ Hz), 3.94–3.68 (m, 8H), 2.90 (s, 3H). $^{13}\text{C NMR}$ (CDCl_3) δ 159.0, 149.6, 148.9, 131.0, 127.1, 122.1, 119.5, 116.4, 115.6, 112.6, 85.0, 81.6, 71.04, 70.8, 70.4, 69.8, 68.0, 30.7. HRMS calcd for $\text{C}_{21}\text{H}_{25}\text{FN}_4\text{O}_3$ (M^+), 400.1911; found, 400.1895.

2-(2-[2-(4-[4-(4-Dimethylaminophenyl)-1H-1,2,3-triazol-1-yl]-phenoxy)ethoxy]ethoxy)ethanol (13b)—In accordance with the procedure for the preparation of **13a**, compound **13b** was prepared from **12a** (0.176 g, 0.5 mmol) as a light yellow solid (0.135 g, 65% yield). ¹H NMR (CDCl₃) δ 7.97 (s, 1H), 7.76 (d, 2H, *J* = 8.7 Hz), 7.64 (d, 2H, *J* = 8.9 Hz), 7.02 (d, 2H, *J* = 8.9 Hz), 6.79 (d, 2H, *J* = 8.6 Hz), 4.17 (t, 2H, *J* = 4.6 Hz), 3.85 (t, 2H, *J* = 4.6 Hz), 3.72–3.60 (m, 8H), 2.99 (s, 6H), 2.61 (br s, 1H). ¹³C NMR (CDCl₃) δ 159.0, 150.5, 148.8, 131.0, 129.4, 126.9, 122.1, 116.5, 115.6, 112.8, 72.6, 71.0, 70.5, 69.8, 68.0, 61.9, 40.7. HRMS calcd for C₂₂H₂₈N₄O₄ (M⁺), 412.2111; found, 412.2106.

4-(1-[4-(2-[2-(2-Fluoroethoxy)ethoxy]ethoxy)phenyl]-1H-1,2,3-triazol-4-yl)-N,N-dimethylbenzenamine (13c)—To a stirred solution of **13b** (0.062 g, 0.15 mmol) in CH₂Cl₂ (5 mL) cooled with an ice bath (0 °C) was added diethylaminosulfur trifluoride (DAST, 0.039 mL, 0.30 mmol) dropwise. After addition, the reaction mixture was maintained at 0 °C for 0.5 h and was submitted to PTLC (EtOAc/hexanes, 70/30) to provide **13c** as a light brown solid (0.013 g, 21%). ¹H NMR (CDCl₃) δ 7.99 (s, 1H), 7.79 (d, 2H, *J* = 8.7 Hz), 7.68 (d, 2H, *J* = 9.0 Hz), 7.06 (d, 2H, *J* = 9.0 Hz), 6.86 (d, 2H, *J* = 8.1 Hz), 4.70 (t, 1H, *J* = 4.2 Hz), 4.46 (t, 1H, *J* = 4.2 Hz), 4.21 (t, 2H, *J* = 4.7 Hz), 3.93–3.68 (m, 8H), 3.02 (s, 6H). ¹³C NMR (CDCl₃) δ 159.2, 148.8, 131.1, 127.1, 122.2, 116.6, 115.7, 113.4, 85.0, 81.7, 71.2, 71.1, 70.9, 70.5, 70.0, 69.8, 68.1, 41.1. HRMS calcd for C₂₂H₂₇N₄O₃ (M⁺), 414.2067; found, 414.2067.

2-(4-[4-(4-Dimethylaminophenyl)-1H-1,2,3-triazol-1-yl]phenoxy)-ethanol (15a)—To a 15 mL two-neck flask were added alkyne **8b** (0.145 g, 1.0 mmol), iodobenzene **14a** (0.264 g, 1.0 mmol), *trans*-N,N'-dimethyl-1,2-cyclohexanediamine (0.024 mL, 0.15 mmol), NaN₃ (0.072 g, 1.1 mmol), sodium ascorbate (0.02 g, 0.10 mmol), CuI (0.019 g, 0.10 mmol), and 3 mL of mixed solvent DMSO and H₂O (5/1 v/v). The reaction mixture was purged by nitrogen for 10 min and then was vigorously stirred at rt for 3 h. After dilution with ice-cold water (15 mL), the solution was filtered and washed with ice-cold water and ice-cold Et₂O. The solid was dried to afford a pale yellow solid **15a** (0.323 g, 98% yield). ¹H NMR [(CD₃)₂-CO] δ 8.64 (s, 1H), 7.87–7.76 (m, 4H), 7.16 (dt, 2H, *J*₁ = 9.1 Hz, *J*₂ = 2.8 Hz), 6.83 (dt, 2H, *J*₁ = 9.0 Hz, *J*₂ = 2.1 Hz), 4.17 (t, 2H, *J* = 4.8 Hz), 4.03–3.88 (m, 3H, -OH, -CH₂), 3.00 (s, 6H). ¹³C NMR [(CD₃)₂CO] δ 160.1, 151.6, 149.4, 131.9, 127.4, 122.5, 120.0, 117.6, 116.4, 113.4, 71.2, 61.4, 61.3, 40.6. HRMS calcd for C₁₈H₂₀N₄O₂ (M⁺), 324.1586; found, 324.1583.

3-(4-[4-(4-Dimethylaminophenyl)-1H-1,2,3-triazol-1-yl]phenoxy)propan-1-ol (15b)—In accordance with the procedure for the preparation of **15a**, compound **15b** was prepared from iodobenzene **14b** (0.278 g, 1.0 mmol) as a pale yellow solid (0.310 g, 92% yield). ¹H NMR [(CD₃)₂CO] δ 8.64 (s, 1H), 7.85–7.78 (m, 4H), 7.15 (dt, 2H, *J*₁ = 9.0 Hz, *J*₂ = 2.7 Hz), 6.83 (d, 2H, *J* = 8.9 Hz), 4.20 (t, 2H, *J* = 6.3 Hz), 3.75 (t, 2H, *J* = 6.0 Hz), 2.99 (s, 6H), 2.00 (pentet, 2H, *J* = 6.2 Hz). ¹³C NMR [(CD₃)₂CO] δ 160.2, 151.6, 131.8, 127.4, 122.6, 120.0, 117.7, 116.3, 113.4, 66.2, 59.1, 58.9, 40.6, 33.4. HRMS calcd for C₁₉H₂₃N₄O₂ (M + H⁺), 339.1822; found, 339.1825.

2-(4-[4-(4-Dimethylaminophenyl)-1H-1,2,3-triazol-1-yl]phenoxy)ethyl 4-Methylbenzenesulfonate (16a)—To a stirred solution of **15b** (0.162 g, 0.5 mmol) in CH₂Cl₂ (5 mL) cooled with an ice bath (0 °C) were added Et₃N (0.35 mL, 2.5 mmol), *p*-toluenesulfonyl chloride (TsCl, 0.143 g, 0.75 mmol) and a catalytic amount of 4-dimethylaminopyridine (DMAP, 0.005 g). After the solution was maintained at 0 °C for 10 min, the ice bath was removed, and the reaction was kept at rt for 3 h and then submitted to standard workup (solvent, CHCl₃/MeOH 90/10). The crude product was purified by FC

(CHCl₃/MeOH 97/3) to provide a pale white solid (0.228 g, 96%). ¹H NMR (CDCl₃) δ 8.01 (s, 1H), 7.86–7.79 (m, 4H), 7.67 (d, 2H, *J* = 9.0 Hz), 7.37 (d, 2H, *J* = 8.5 Hz), 6.96–6.91 (m, 4H), 4.44–4.40 (m, 2H), 4.25–4.21 (m, 2H), 3.05 (s, 6H), 2.47 (s, 3H). ¹³C NMR (CDCl₃) δ 158.3, 148.8, 145.3, 132.8, 131.3, 130.0, 128.1, 126.9, 122.2, 116.8, 115.6, 113.2, 68.1, 66.0, 40.8, 21.7.

3-(4-[4-(4-Dimethylaminophenyl)-1*H*-1,2,3-triazol-1-yl]phenoxy)propyl 4-methylbenzenesulfonate (16b)—In accordance with the procedure for the preparation of **16a**, compound **16b** was prepared from alcohol **15c** (0.169 g, 0.5 mmol) as a pale white solid (0.221 g, 90% yield). ¹H NMR [(CD₃)₂CO] δ 8.65 (s, 1H), 7.84–7.77 (m, 6H), 7.40 (d, 2H, *J* = 8.0 Hz), 7.03 (dt, 2H, *J*₁ = 9.0 Hz, *J*₂ = 2.8 Hz), 6.83 (d, 2H, *J* = 8.9 Hz), 4.29 (t, 2H, *J* = 6.0 Hz), 4.08 (t, 2H, *J* = 5.9 Hz), 2.99 (s, 6H), 2.38 (s, 3H), 2.16 (pentet, 2H, *J* = 6.0 Hz). ¹³C NMR [(CD₃)₂CO] δ 159.6, 151.6, 145.9, 131.0, 128.7, 127.4, 126.1, 122.5, 120.0, 117.7, 116.2, 113.4, 68.2, 64.7, 40.6, 21.6.

4-(1-[4-(2-Fluoroethoxy)phenyl]-1*H*-1,2,3-triazol-4-yl)-*N,N*-dimethylbenzenamine (17a)—To a solution of tosylate **16a** (0.096 g, 0.20 mmol) in THF (1 mL) was added TBAF solution (1.0 M in THF, 1.0 mL). The reaction solution was heated in the microwave reactor at 110 °C for 0.5 h. After cooling and standard workup with EtOAc, the residue was purified by PTLC (EtOAc/hexanes, 50/50) to afford **8c** as a light brown solid (0.052 g, 80%). ¹H NMR [(CD₃)₂CO] δ 8.65 (s, 1H), 7.90–7.78 (m, 4H), 7.20 (dt, 2H, *J*₁ = 9.1 Hz, *J*₂ = 2.8 Hz), 6.83 (d, 2H, *J* = 8.9 Hz), 4.96–4.923 (m, 1H), 4.72–4.68 (m, 1H), 4.48–4.44 (m, 1H), 4.33–4.29 (m, 1H), 3.00 (s, 6H). ¹³C NMR [(CD₃)₂CO] δ 159.6, 151.7, 149.4, 132.3, 127.4, 122.6, 120.0, 117.7, 116.4, 113.4, 84.6, 81.3, 69.0, 68.6, 40.6. HRMS calcd for C₁₈H₁₉FN₄O (M⁺), 326.1543; found, 326.1532.

4-(1-[4-(3-Fluoropropoxy)phenyl]-1*H*-1,2,3-triazol-4-yl)-*N,N*-dimethylbenzenamine (17b)—In accordance with the procedure for the preparation of **17a**, compound **17b** was prepared from tosylate **16b** (0.099 g, 0.2 mmol) as a white solid (0.068 g, 100% yield). ¹H NMR [(CD₃)₂CO] δ 8.64 (s, 1H), 7.88–7.78 (m, 6H), 7.18 (dt, 2H, *J*₁ = 6.8 Hz, *J*₂ = 2.8 Hz), 6.83 (d, 2H, *J* = 8.9 Hz), 4.79 (t, 1H, *J* = 5.9 Hz), 4.56 (t, 1H, *J* = 5.9 Hz), 4.23 (t, 2H, *J* = 6.2 Hz), 2.99 (s, 6H), 2.28 (pentet, 1H, *J* = 6.0 Hz), 2.15 (pentet, 1H, *J* = 6.0 Hz). ¹³C NMR [(CD₃)₂CO] δ 159.8, 151.6, 149.4, 132.1, 127.4, 122.6, 120.0, 117.7, 116.3, 113.4, 83.1, 79.9, 65.0, 40.6, 31.4, 31.0. HRMS calcd for C₁₉H₂₂FN₄O (M + H⁺), 341.1779; found, 341.1776.

Radiolabeling

(1) Radioiodination—The radioiodinated compounds [¹²⁵I]**10a** and [¹²⁵I]**10b** were prepared via iododestannylation reactions from the corresponding tributyltin precursors **11a** and **11b** according to the method described previously.^{44,45} Hydrogen peroxide (50 μL, 3% w/v) was added to a mixture of 50 μL of the tributyltin precursor (4 μg/μL EtOH), 50 μL of 1 N HCl, and [¹²⁵I]-NaI (1–5 mCi purchased from Perkin-Elmer) in a sealed vial. The reaction was allowed to proceed for 10 min at room temperature and terminated by the addition of 100 μL of saturated NaHSO₃ solution. The reaction mixture neutralized with 1.5 mL of saturated NaHCO₃ solution was loaded on a small preconditioned C-4 minicolumn. After sequential rinsing with 10% and 20% EtOH solutions, the desired products [¹²⁵I]**10a** and [¹²⁵I]**10b** were obtained. The radiochemical purity was checked by HPLC on a reversed-phase column (Phenomenex Gemini C18 analytical column, 4.6 × 250 mm, 5 μm, CH₃CN/ammonium formate buffer (1 mM) 8/2; flow rate 0.5 mL/min). The no-carrier-added products were stored at –20 °C up to 6 weeks for animal studies, homogenate binding, and autoradiography studies.

(2) Radiofluorination— ^{18}F Fluoride was produced by the JSW typeBC3015 cyclotron via O-18(p,n) F-18 reaction and passed through a Sep-Pak Light QMA cartridge (Waters) as an aqueous solution in ^{18}O -enriched water. The cartridge was dried by airflow, and the F-18 activity was eluted with 1.3 mL of Kryptofix 222 (K222)/ K_2CO_3 solution (11 mg of K222 and 2.6 mg of K_2CO_3 in $\text{CH}_3\text{CN}/\text{H}_2\text{O}$ 1.12/0.18). The solvent was removed at 120 °C under an argon stream. The residue was azeotropically dried with 1 mL of anhydrous CH_3CN twice at 120 °C under a nitrogen stream. A solution of tosylate precursor **16a** or **16b** (2 mg) in DMSO (0.2 mL) was added to the reaction vessel containing the dried F-18 activities. The mixture was heated at 120 °C for 4 min. Water (5 mL) was added and the mixture was passed through a preconditioned Oasis HLB cartridge (3 cm^3) (Waters). The cartridge was washed with 10 mL of water and the labeled compound was eluted with 2 mL of CH_3CN . The eluted compound was purified by HPLC [Phenomenex Gemini C18 semipreparative column (10 \times 250 mm, 5 μm), $\text{CH}_3\text{CN}/\text{water}$ 7/3, flow rate 3 mL/min, t_{R} = 11 min]. The radiochemical purity and specific activity were determined by analytical HPLC (Phenomenex Gemini C18 analytical column (4.6 \times 250 mm, 5 μm), $\text{CH}_3\text{CN}/\text{ammonium formate buffer}$ (10 mM) 8/2; flow rate 1 mL/min; t_{R} = 4.8 min for ^{18}F **17a**, 5.7 min for ^{18}F **17b**). Specific activity was estimated by comparing the UV peak intensity of the purified F-18 labeled compound with reference nonradioactive compound of known concentration.

Preparation of Brain Tissue Homogenates

AD postmortem brain tissues were obtained from the University of Washington Alzheimer's Disease Research Center. The neuropathological diagnosis was confirmed by current criteria (NIA-Reagan Institute Consensus Group, 1997). Homogenates were then prepared from dissected gray matters from four pooled AD patients in phosphate-buffered saline (PBS, pH 7.4) at the concentration of approximately 100 mg of wet tissue/mL (motor-driven glass homogenizer with setting of 6 for 30 s). The homogenates were aliquoted into 1-mL portions and stored at -70 °C for up to 2 years without loss of binding signal.

Binding Studies

The ligand ^{125}I **2**, with 2200 Ci/mmol specific activity and greater than 95% radiochemical purity, was prepared by the standard iododestannylation reaction and purified on a simplified C-4 minicolumn as described previously. Binding assays were carried out in 12 \times 75 mm borosilicate glass tubes. For competition studies, the reaction mixture contained 50 μL of pooled AD brain homogenates (20–50 μg), 50 μL of ^{125}I **2** (0.04–0.06 nM diluted in PBS) and 50 μL of inhibitors (10^{-5} – 10^{-10} M diluted serially in PBS containing 0.1% bovine serum albumin) in a final volume of 1 mL. Nonspecific binding was defined in the presence of 600 nM **2** in the same assay tubes. The mixture was incubated at 37 °C for 2 h, and the bound and free radioactivity were separated by vacuum filtration through Whatman GF/B filters by use of a Brandel M-24R cell harvester followed by 2 \times 3 mL washes of PBS at room temperature. Filters containing the bound ^{125}I ligand were counted in a γ -counter (Packard 5000) with 70% counting efficiency. Under the assay conditions, the fraction that was nonspecifically bound was less than 20% of the total radioactivity. The results of inhibition experiments were subjected to nonlinear regression analysis by use of equilibrium binding data analysis, with which K_{i} values were calculated.

Similarly, the specific binding of radioiodinated and radiofluorinated ligands (0.06 nM for ^{125}I probe and 0.5 nM for ^{18}F probe) to homogenates, prepared from the gray and white matters of AD and control brain tissues, were carried out as described above. Nonspecific binding was determined in the presence of 2 μM of the corresponding nonradioactive probes.

In Vitro autoradiography

To compare different probes using similar sections of human brain tissue, human macroarray brain sections from six confirmed AD cases and one control subject were assembled. The presence and localization of plaques on the sections was confirmed with immunohistochemical staining with monoclonal A β antibody 4G8 (Sigma). The frozen sections were incubated with [¹²⁵I] and [¹⁸F]tracers (200 000–250 000 cpm/200 μ L) for 1 h at room temperature. The sections were then dipped in saturated LiOH in 40% EtOH (two 2-min washes) and washed with 40% EtOH (one 2-min wash), followed by rinsing with water for 30 s. After drying, the I-125 or F-18 labeled sections were exposed to Kodak Biomax MR film overnight.

Organ Distribution in Normal Mice

While the mice were under isoflurane anesthesia, 0.15 mL of a 0.1% bovine serum albumin solution containing [¹²⁵I] or [¹⁸F]tracers (5–10 μ Ci) was injected directly into the tail vein of ICR mice (22–25 g, male). The mice ($n = 3$ for each time point) were sacrificed by cervical dislocation at designated time points postinjection. The organs of interest were removed and weighed, and the radioactivity was counted with an automatic γ -counter. The percentage dose per organ was calculated by a comparison of the tissue counts to suitably diluted aliquots of the injected material. The total activity of the blood was calculated under the assumption that it is 7% of the total body weight. The % ID/g of samples was calculated by comparing the sample counts with the count of the diluted initial dose.

Partition Coefficient

Partition coefficients were measured by mixing the [¹²⁵I] or [¹⁸F] tracer with 3 g each of 1-octanol and buffer (0.1 M phosphate, pH 7.4) in a test tube. The test tube was vortexed for 3 min at room temperature, followed by centrifugation for 5 min. Two weighed samples (0.5 g each) from the 1-octanol and buffer layers were counted in a well counter. The partition coefficient was determined by calculating the ratio of cpm/g of 1-octanol to that of buffer. Samples from the 1-octanol layer were repartitioned until consistent partitions of coefficient values were obtained. The measurement was done in triplicate and repeated three times.

Supplementary Material

Refer to Web version on PubMed Central for supplementary material.

Acknowledgments

This work was supported by grants from the National Institutes of Health (AG022559 to H.F.K and AG-021868 to M.P.K). We thank Dr. Carita Huang for her editorial assistance.

References

1. Selkoe DJ. Imaging Alzheimer's amyloid. *Nat Biotechnol.* 2000; 18:823–824. [PubMed: 10932146]
2. Hardy J. Alzheimer's disease: The amyloid cascade hypothesis: An update and reappraisal. *J Alzheimers Dis.* 2006; 9:151–3. [PubMed: 16914853]
3. Goedert M, Spillantini MG. A century of Alzheimer's disease. *Science.* 2006; 314:777–81. [PubMed: 17082447]
4. Mathis CA, Klunk WE, Price JC, DeKosky ST. Imaging technology for neurodegenerative diseases: progress toward detection of specific pathologies. *Arch Neurol.* 2005; 62:196–200. [PubMed: 15710847]
5. Mathis CA, Wang Y, Klunk WE. Imaging β -amyloid plaques and neurofibrillary tangles in the aging human brain. *Curr Pharm Des.* 2004; 10:1469–1492. [PubMed: 15134570]

6. Verhoeff NP, Wilson AA, Takeshita S, Trop L, Hussey D, Singh K, Kung HF, Kung MP, Houle S. In vivo imaging of Alzheimer disease beta-amyloid with [¹¹C]SB-13 PET. *Am J Geriatr Psychiatry*. 2004; 12:584–595. [PubMed: 15545326]
7. Ono M, Wilson A, Nobrega J, Westaway D, Verhoeff P, Zhuang ZP, Kung MP, Kung HF. ¹¹C-labeled stilbene derivatives as Abeta-aggregate-specific PET imaging agents for Alzheimer's disease. *Nucl Med Biol*. 2003; 30:565–571. [PubMed: 12900282]
8. Zhuang ZP, Kung MP, Wilson A, Lee CW, Plossl K, Hou C, Holtzman DM, Kung HF. Structure-activity relationship of imidazo[1,2-*a*]pyridines as ligands for detecting β -amyloid plaques in the brain. *J Med Chem*. 2003; 46:237–243. [PubMed: 12519062]
9. Kung MP, Hou C, Zhuang ZP, Skovronsky D, Kung HF. Binding of two potential imaging agents targeting amyloid plaques in postmortem brain tissues of patients with Alzheimer's disease. *Brain Res*. 2004; 1025:89–105.
10. Mathis CA, Wang Y, Holt DP, Huang G-f, Debnath ML, Klunk WE. Synthesis and Evaluation of ¹¹C-Labeled 6-Substituted 2-Arylbenzothiazoles as Amyloid Imaging Agents. *J Med Chem*. 2003; 46:2740–2754. [PubMed: 12801237]
11. Klunk WE, Engler H, Nordberg A, Wang Y, Blomqvist G, Holt DP, Bergstrom M, Savitcheva I, Huang G-f, Estrada S, Ausen B, Debnath ML, Barletta J, Price JC, Sandell J, Lopresti BJ, Wall A, Koivisto P, Antoni G, Mathis CA, Langstrom B. Imaging Brain Amyloid in Alzheimer's Disease with Pittsburgh Compound-B. *Ann Neurol*. 2004; 55:306–319. [PubMed: 14991808]
12. Small GW, Kepe V, Ercoli LM, Siddarth P, Bookheimer SY, Miller KJ, Lavretsky H, Burggren AC, Cole GM, Vinters HV, Thompson PM, Huang SC, Satyamurthy N, Phelps ME, Barrio JR. PET of brain amyloid and tau in mild cognitive impairment. *N Engl J Med*. 2006; 355:2652–63. [PubMed: 17182990]
13. Agdeppa ED, Kepe V, Liu J, Flores-Torres S, Satyamurthy N, Petric A, Cole GM, Small GW, Huang SC, Barrio JR. Binding characteristics of radiofluorinated 6-dialkylamino-2-naphthylethylidene derivatives as positron emission tomography imaging probes for β -amyloid plaques in Alzheimer's disease. *J Neurosci*. 2001; 21:RC189. [PubMed: 11734604]
14. Lockhart A. Imaging Alzheimer's disease pathology: one target many ligands. *Drug Discovery Today*. 2006; 11:1093–9. [PubMed: 17129828]
15. Okamura N, Suemoto T, Furumoto S, Suzuki M, Shimadzu H, Akatsu H, Yamamoto T, Fujiwara H, Nemoto M, Maruyama M, Arai H, Yanai K, Sawada T, Kudo Y. Quinoline and benzimidazole derivatives: candidate probes for in vivo imaging of tau pathology in Alzheimer's disease. *J Neurosci*. 2005; 25:10857–62. [PubMed: 16306398]
16. Shimadzu H, Suemoto T, Suzuki M, Shiomitsu T, Okamura N, Kudo Y, Sawada T. Novel probes for imaging amyloid- β : F-18 and C-11 labeling of 2-(4-aminostyryl)benzoxazole derivatives. *J Lab Compds Radiopharm*. 2004; 47:181–190.
17. Okamura N, Suemoto T, Shimadzu H, Suzuki M, Shiomitsu T, Akatsu H, Yamamoto T, Staufenbiel M, Yanai K, Arai H, Sasaki H, Kudo Y, Sawada T. Styrylbenzoxazole derivatives for in vivo imaging of amyloid plaques in the brain. *J Neurosci*. 2004; 24:2535–2541. [PubMed: 15014129]
18. Zhang W, Kung MP, Oya S, Hou C, Kung HF. (¹⁸F)-labeled styrylpyridines as PET agents for amyloid plaque imaging. *Nucl Med Biol*. 2007; 34:89–97. [PubMed: 17210465]
19. Cai L, Innis RB, Pike VW. Radioligand Development for PET Imaging of beta-Amyloid (Abeta)-Current Status. *Curr Med Chem*. 2007; 14:19–52. [PubMed: 17266566]
20. Chandra R, Oya S, Kung MP, Hou C, Jin LW, Kung HF. New diphenylacetylenes as probes for PET imaging of amyloid plaques. *J Med Chem*. 2007 In Press.
21. Zhuang ZP, Kung MP, Kung HF. Synthesis of Biphenyltrienes as Probes for β -Amyloid Plaques. *J Med Chem*. 2006; 49:2841–2844. [PubMed: 16640346]
22. Chandra R, Kung MP, Kung HF. Design, synthesis, and structure-activity relationship of novel thiophene derivatives for beta-amyloid plaque imaging. *Bioorg Med Chem Lett*. 2006; 16:1350–2. [PubMed: 16325402]
23. Huisgen, R. Introduction, survey, mechanism. In: Padwa, A., editor. 1,3-Dipolar cycloaddition. Vol. 1. John Wiley & Sons; New York: 1984. p. 76-147.

24. Sharpless KB, Manetsch R. In situ click chemistry: a powerful means for lead discovery. *Expert Opin Drug Discovery*. 2006; 1:525–538.
25. Roper, S.; Kolb, HC. Click chemistry for drug discovery. In: Jahnke, W.; Erlanson, DA., editors. *Fragment-Based Approaches in Drug Discovery*. Vol. 34. Wiley–VCH; Weinheim, Germany: 2006. p. 313–339.
26. Fokin VV, Sharpless KB. A practical and highly efficient aminohydroxylation of unsaturated carboxylic acids. *Angew Chem, Int Ed*. 2001; 40:3455–3457.
27. Liang B, Huang M, You Z, Xiong Z, Lu K, Fathi R, Chen J, Yang Z. Pd-catalyzed copper-free carbonylative Sonogashira reaction of aryl iodides with alkynes for the synthesis of alkynyl ketones and flavones by using water as a solvent. *J Org Chem*. 2005; 70:6097–100. [PubMed: 16018709]
28. Rostovtsev VV, Green LG, Fokin VV, Sharpless KB. A stepwise Huisgen cycloaddition process: copper(I)-catalyzed regioselective “ligation” of azides and terminal alkynes. *Angew Chem, Int Ed*. 2002; 41:2596–9.
29. Pagliai F, Pirali T, Del Grosso E, Di Brisco R, Tron GC, Sorba G, Genazzani AA. Rapid Synthesis of Triazole-Modified Resveratrol Analogues via Click Chemistry. *J Med Chem*. 2006; 49:467–470. [PubMed: 16420033]
30. Mocharla VP, Colasson B, Lee LV, Roper S, Sharpless KB, Wong CH, Kolb HC. In situ click chemistry: enzyme-generated inhibitors of carbonic anhydrase II. *Angew Chem, Int Ed*. 2004; 44:116–20.
31. Yan ZY, Niu YN, Wei HL, Wu LY, Zhao YB, Liang YM. Combining proline and ‘click chemistry’: a class of versatile organocatalysts for the highly diastereo- and enantioselective Michael addition in water. *Tetrahedron: Asymmetry*. 2007; 17:3288–3293.
32. Kolb HC, Finn MG, Sharpless KB. Click Chemistry: Diverse Chemical Function from a Few Good Reactions. *Angew Chem, Int Ed*. 2001; 40:2004–2021.
33. Kolb HC, Sharpless KB. The growing impact of click chemistry on drug discovery. *Drug Discovery Today*. 2003; 8:1128–37. [PubMed: 14678739]
34. Wang J, Sui G, Mocharla VP, Lin RJ, Phelps ME, Kolb HC, Tseng HR. Integrated microfluidics for parallel screening of an in situ click chemistry library. *Angew Chem, Int Ed*. 2006; 45:5276–81.
35. Kolb, HC.; Mocharla, VP.; Walsh, JC. In situ click chemistry method for screening high affinity molecular imaging probes. U.S. Patent 2006-US16428 (2006116736), 20060427. 2006.
36. Kolb, HC.; Walsh, JC.; Chen, K. Click chemistry method for synthesizing ¹⁸F-labeled AZT as molecular imaging probes. U.S. Patent 2006-US16088 (2006116629), 20060427. 2006.
37. Marik J, Sutcliffe JL. Click for PET: rapid preparation of [¹⁸F]-fluoropeptides using CuI catalyzed 1,3-dipolar cycloaddition. *Tetrahedron Lett*. 2006; 47:6681–6684.
38. Mindt TL, Struthers H, Brans L, Anguelov T, Schweinsberg C, Maes V, Tourwe D, Schibli R. \ “Click to Chelate\”: Synthesis Installation of Metal Chelates into Biomolecules in a Single Step. *J Am Chem Soc*. 2006; 128:15096–15097. [PubMed: 17117854]
39. Dijkgraaf I, Rijnders AY, Soede A, Dechesne AC, van Esse GW, Brouwer AJ, Corstens FH, Boerman OC, Rijkers DT, Liskamp RM. Synthesis of DOTA-conjugated multivalent cyclic-RGD peptide dendrimers via 1,3-dipolar cycloaddition and their biological evaluation: implications for tumor targeting and tumor imaging purposes. *Org Biomol Chem*. 2007; 5:935–44. [PubMed: 17340009]
40. Feldman AK, Colasson B, Fokin VV. One-Pot Synthesis of 1,4-disubstituted 1,2,3-triazoles from in situ generated azides. *Org Lett*. 2004; 6:3897–3899. [PubMed: 15496058]
41. Andersen J, Bolvig S, Liang X. Efficient one-pot synthesis of 1-aryl 1,2,3-triazoles from aryl halides and terminal alkynes in the presence of sodium azide. *Synlett*. 2005:2941–2947.
42. Stephenson KA, Chandra R, Zhuang ZP, Hou C, Oya S, Kung MP, Kung HF. Fluoro-pegylated (FPEG) Imaging Agents Targeting Abeta Aggregates. *Bioconjugate Chem*. 2007; 18:238–46.
43. Zhang W, Oya S, Kung MP, Hou C, Maier DL, Kung HF. F-18 PEG Stilbenes as PET Imaging Agents Targeting A β Aggregates in the Brain. *Nucl Med Biol*. 2005; 32:799–809. [PubMed: 16253804]

44. Kung MP, Hou C, Zhuang ZP, Cross AJ, Maier DL, Kung HF. Characterization of IMPY as a potential imaging agent for β -amyloid plaques in double transgenic PSAPP mice. *Eur J Nucl Med Mol Imaging*. 2004; 31:1136–1145. [PubMed: 15007564]
45. Kung MP, Hou C, Oya S, Mu M, Acton PD, Kung HF. Characterization of [123 I]IDAM as a novel single-photon emission tomography tracer for serotonin transporters. *Eur J Nucl Med*. 1999; 26:844–53. [PubMed: 10436197]

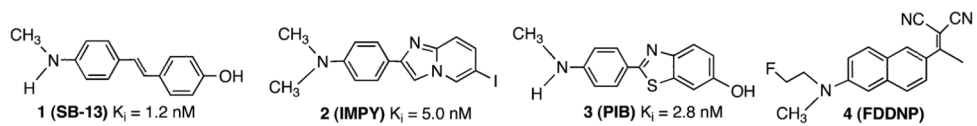


Figure 1. Structures of four agents (**1–4**) reported for imaging A β aggregates in the brain. K_i values indicate the in vitro binding affinities to AD brain homogenates.⁹

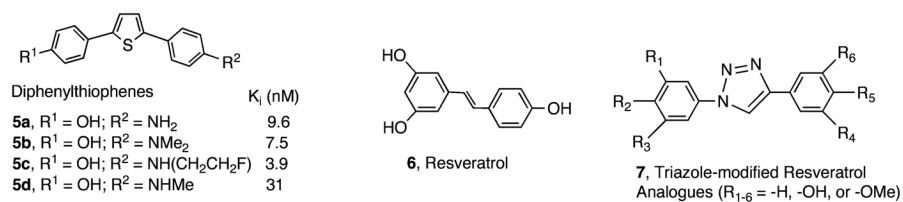


Figure 2.

Diphenylthiophenes, a tricyclic ring system, also displayed excellent binding affinities to A β aggregates ($K_i = 3.9$ – 31 nM). It was recently reported²⁹ that, by use of click chemistry, **6** was modified. The tricyclic structure diphenyltriazoles, **7**, retained many aspects of interesting antioxidant properties. Using the same concept, the click chemistry derivatives of **1** led to the formation of tricyclic diphenyltriazoles that showed excellent high binding affinities to A β aggregates comparable to those observed for **1** and **5**.

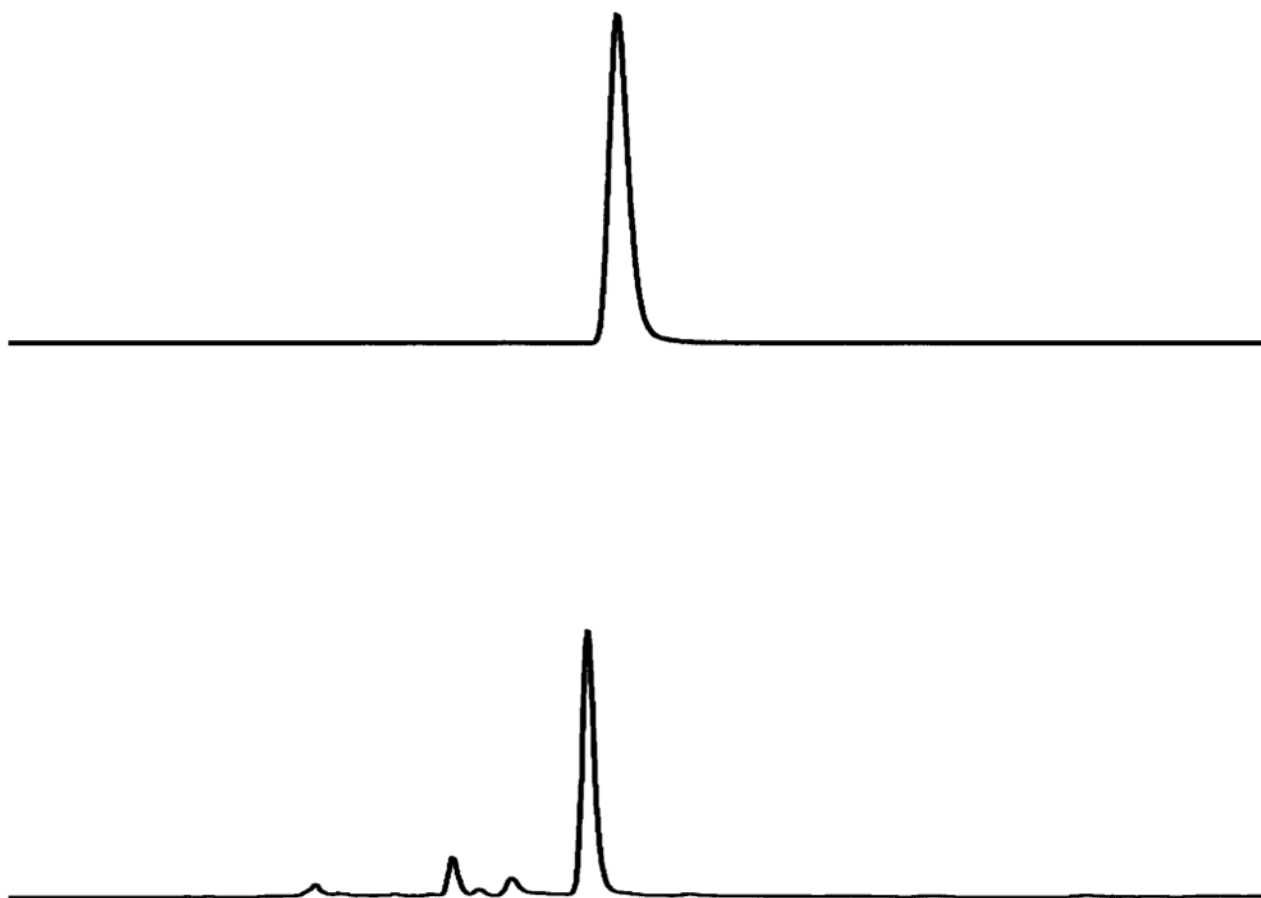


Figure 3. HPLC profiles of [^{18}F]**17a** (top) and **17a** (bottom). HPLC conditions: Agilent 1100 series; Gemini C-18 analytical column (4.6×250 mm, $5 \mu\text{m}$), $\text{CH}_3\text{CN}/\text{ammonium formate}$ (10 mM) 8/2, 1 mL/min, 265 nm, t_{R} = (UV) 4.5 min, (γ) 4.8 min. The slight difference in retention time between the radioactive peak and the UV peak is due to the configuration of the detector system).

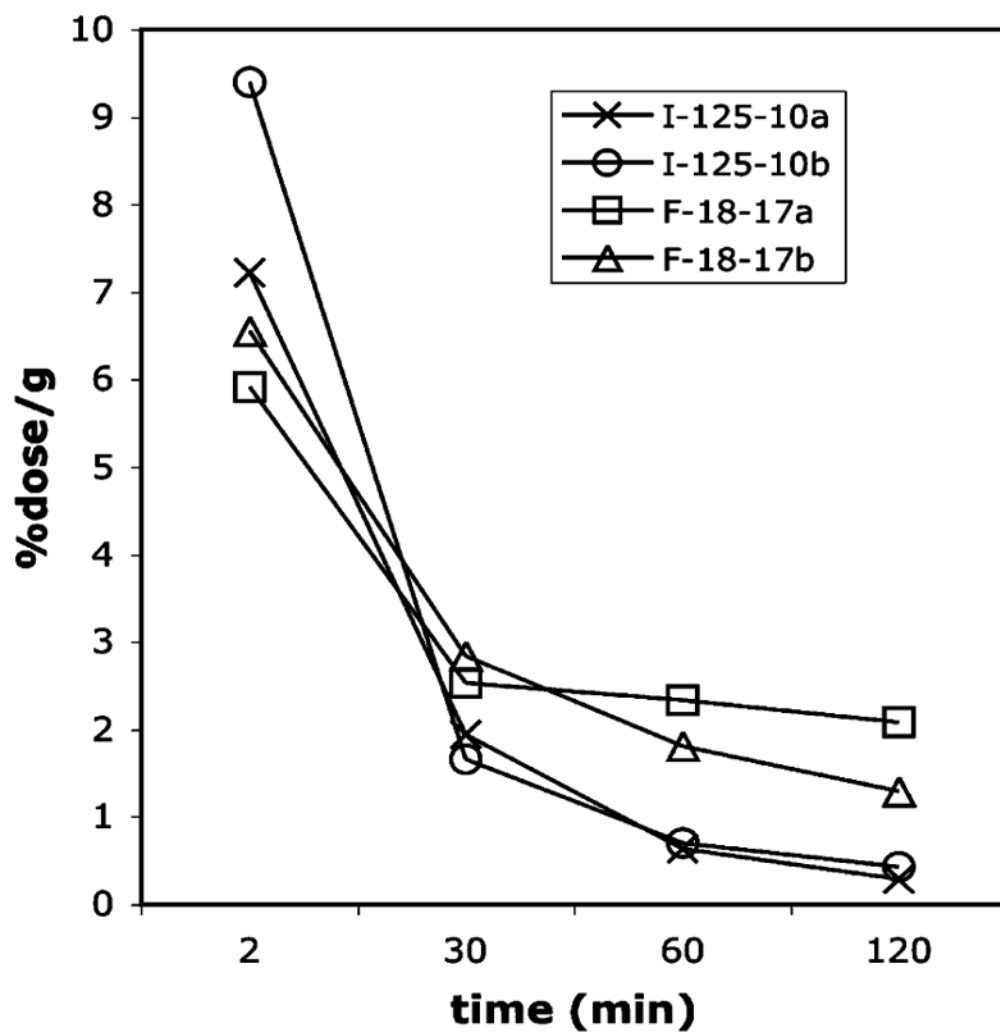


Figure 4. Brain uptakes and washouts of radiolabeled triazole probes in normal mice. Data are presented as % ID/g of three mice \pm standard deviation.

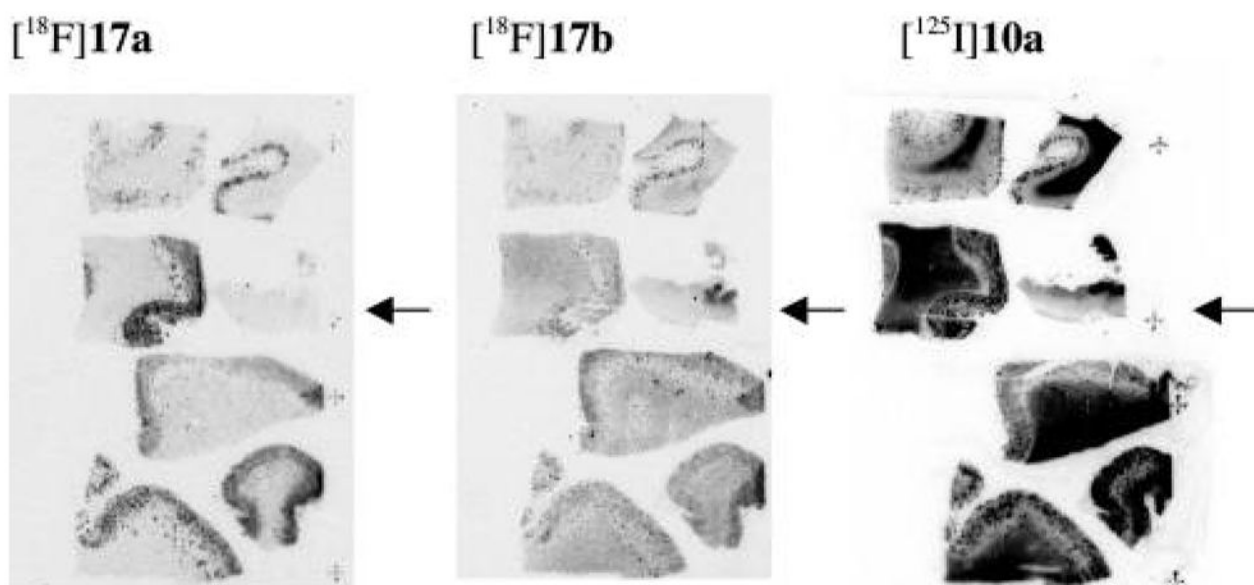


Figure 5.

In vitro film autoradiography of macroarray brain sections constructed from six AD and one control (marked by arrowhead) cases. The $A\beta$ plaques were clearly visualized with low background labeling with the two radiofluorinated probes $[^{18}\text{F}]\mathbf{17a}$ and $[^{18}\text{F}]\mathbf{17b}$. High white matter labeling was observed with the iodinated probe $[^{125}\text{I}]\mathbf{10a}$ in addition to plaque labeling.

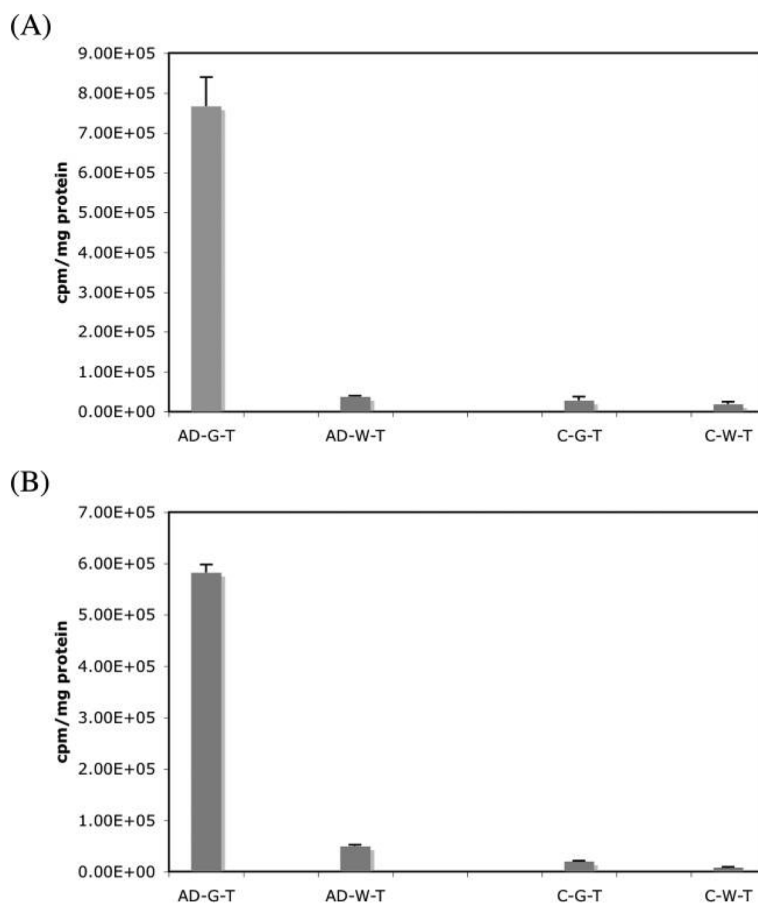
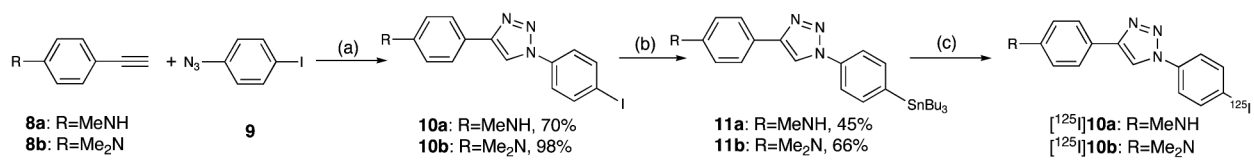
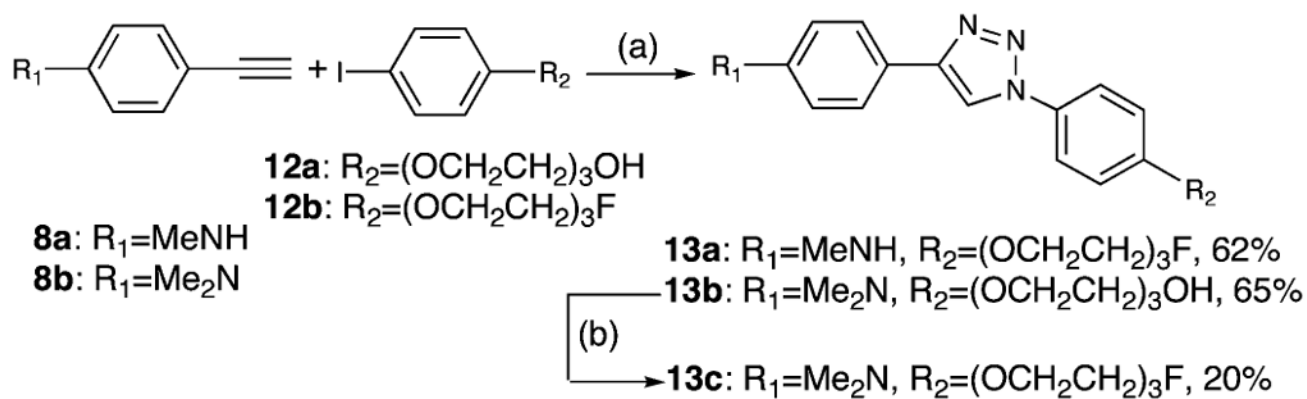


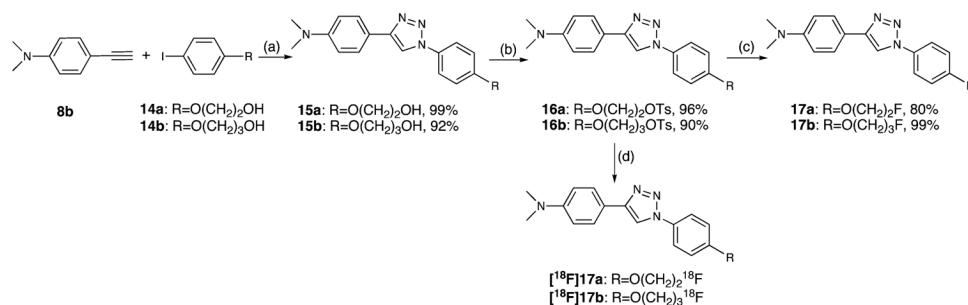
Figure 6. Specific binding of (A) $[^{125}\text{I}]\mathbf{10a}$ and (B) $[^{18}\text{F}]\mathbf{17a}$ to pooled AD and control brain tissue homogenates. Gray and white matter was dissected from the cortical regions. High specific binding was detected mainly in the gray matter of AD brain. Relatively low binding was measured in the white matter homogenates of AD brain as well as in gray and white matter homogenates of the control brain.

**Scheme 1a.**

^a Reagents and conditions: (a) CuSO₄, sodium ascorbate, *t*-BuOH/H₂O, rt, 24 h; (b) (Bu₃Sn)₂, Pd(PPh₃)₄, toluene, 100 °C, 4 h; (c) H₂O₂, Na¹²⁵I, HCl, EtOH.

**Scheme 2a.**

^a Reagents and conditions: (a) Na_2CO_3 , sodium ascorbate, CuSO_4 , L-proline, NaN_3 , DMSO/ H_2O , 65 °C, 24 h; (b) DAST, CH_2Cl_2 , 0 °C, 0.5 h.

**Scheme 3a.**

^a Reagents and conditions: (a) NaN₃, *trans*-*N,N'*-dimethyl-1,2-cyclohexanediamine, CuI, sodium ascorbate, DMSO/H₂O, rt, 3 h; (b) TsCl, Et₃N, DMAP, CH₂Cl₂, 0 °C to rt, 3 h; (c) TBAF, THF, 110 °C, 0.5 h, microwave heating; (d) [¹⁸F]HF, K222, K₂CO₃, DMSO, 120 °C, 4.0 min.

Table 1

Potencies (K_i) of Compounds Competing with [125 I]2 Binding to Amyloid Plaques in AD Brain Homogenates^a

compound	K_i (nM \pm SEM)
10a	4.0 \pm 0.4
10b	8.0 \pm 1.6
13a	30.0 \pm 6.0
13b	16.5 \pm 3.3
13c	8.4 \pm 1.7
15a	10.0 \pm 2.0
15b	75 \pm 10
17a	5.0 \pm 1.0
17b	6.2 \pm 1.2

^aEach value was determined three times with duplicates for each measurement.